Entropy and Fluid−Fluid Separation in Nonadditive Hard-Sphere Mixtures: The Asymmetric Case

ARTICLE *in* THE JOURNAL OF PHYSICAL CHEMISTRY B · JANUARY 2002

Impact Factor: 3.3 · DOI: 10.1021/jp013150k

2 AUTHORS, INCLUDING:

Franz Saija
Italian National Research Council
92 PUBLICATIONS **1,099** CITATIONS

BATCH: jp2c27 USER: jld69 DIV: @xyv04/data1/CLS_pj/GRP_jp/JOB_i07/DIV_jp013150k DATE: January 2, 2002

Entropy and Fluid−Fluid Separation in Nonadditive Hard-Sphere Mixtures: The Asymmetric Case

F. Saija*,† and P. V. Giaquinta*,‡

Istituto di Tecniche Spettroscopiche del CNR, Via La Farina 237, 98123, Messina, Italy, and Istituto Nazionale per la Fisica della Materia, Unità di Ricerca di Messina, and Dipartimento di Fisica, Università degli Studi di Messina, Contrada Papardo, 98166 Messina, Italy

Received: August 14, 2001; In Final Form: October 22, 2001

We report Monte Carlo simulation results for the thermodynamic and structural properties of binary nonadditive mixtures of hard spheres with not too dissimilar sizes. The simulations were carried out over a range of parameters where fluid−fluid separation is known to compete with freezing. We investigated the onset of structural ordering in a one-phase scheme as that provided by the residual multiparticle entropy, an integrated measure of the weight of spatial correlations involving more than two particles in the configurational entropy of the system. This approach has been already tested in the symmetric case [Saija, F.; Pastore, G.; Giaquinta, P. V. *J. Phys. Chem. B* **1998**, *102*, 10368]. The present study confirms the indication that a rather small amount of nonadditivity may significantly influence the phase behavior of the mixture also in a thermodynamic regime where osmotic depletion effects do not play a leading role.

1. Introduction

A binary mixture of hard spheres is an established prototype model for understanding basic phenomena in the equilibrium statistical mechanics of complex fluids. This model is characterized by two like collision diameters (σ_{11}, σ_{22}) and by an interspecies diameter $\sigma_{12} = {}^1/_2(\sigma_{11} + \sigma_{22})(1 + \Delta)$, where the dimensionless parameter Δ accounts for deviations of unlike excluded-volume interactions from additivity. As is well-known, in a real system such repulsive effects are associated with the overlap between the electron clouds of colliding molecules. Even in a rare-gas mixture, the Lorentz rule ($\Delta = 0$) is not systematically satisfied.[1] Deviations from additivity may be expected to occur at high pressures. They also become manifest in the "effective" interactions that characterize some complex polydisperse fluids such as colloid−polymer mixtures.[2] In general, the thermodynamic and phase-stability properties of a system turn out to be rather sensitively affected by even a modest degree of nonadditivity.

In a previous paper we have analyzed the thermodynamic behavior of a mixture of equal-sized hard spheres with an interspecies diameter larger than that of each component,[3] focusing on the indications of phase separation that are provided by a one-phase method based on the multiparticle correlation expansion of the configurational entropy.[4] This approach, which just requires the knowledge of pair correlations in the homogeneous phase, was originally proposed in ref 5 and then extended to multicomponent fluids[6] and to lattice systems[7] as well. The method has proven successful for a variety of model fluids in that it usually gives a rather neat indication of the emergence of ordering processes in the system in three as well as in two dimensions.[8,9]

A bidisperse mixture of hard spheres may exist in a surprisingly rich variety of both ordered and disordered phases whose formation is uniquely driven by entropic effects depending on the diameter ratio $q = \sigma_{22}/\sigma_{11}$ (we conventionally identify larger particles as species 1 in such a way that $q \leq 1$), on the deviation from additivity Δ, and on the mole fractions x_1 and $x_2 = 1 - x_1$ of the two species.[10] An additive hard-sphere mixture exhibits stable solid phases at high enough densities. As the size ratio decreases from 1 to 0.85, the shape of the phase diagram changes from a spindle to an azeotropic type until a eutectic point eventually stems.[11,12] More complex superlattice structures are stable for intermediate values of the size ratio ($q < 0.6$).[13] For even more asymmetric sizes ($q < 0.3$), the mixture tends to phase-separate, as a result of osmotic depletion effects, when the larger-particle species is sufficiently dilute.[14] However, Monte Carlo (MC) simulations have also shown that demixing is preempted by the freezing of the species at lower concentration.[15]

In a nonadditive hard-sphere (NAHS) mixture, the dominant mechanism underlying phase separation is different. First of all, the sign of Δ is critical as to the type of thermodynamic behavior that is exhibited by the mixture. For $\Delta < 0$ the model shows a tendency toward heterocoordination and is able to reproduce the large compositional fluctuations that are observed in some liquid and amorphous mixtures.[16−18] On the contrary, for $\Delta > 0$, even an equal-sized NAHS mixture exhibits phase separation at high densities. This phenomenon is due to the extra repulsion between unlike spheres, which overcomes the disordering effect of the thermal motion. The equal-diameter case has been investigated with a variety of theoretical methods.[19−27] A number of phenomenological equations of state have been proposed as well.[28−30] Furthermore, numerical simulation studies have been performed for both negative and positive values of the nonadditivity parameter.[31−34]

So far, the asymmetric case has been studied much less than the symmetric one. The first simulation experiment of a NAHS mixture with not too dissimilar diameters of the two species was carried out by Rovere and Pastore,[35] who traced the phase diagram by means of the Gibbs ensemble Monte Carlo (GEMC)

* E-mail saija@me.cnr.it or Paolo.Giaquinta@unime.it.
† Istituto di Tecniche Spettroscopiche del CNR.
‡ Istituto Nazionale per la Fisica della Materia, Unità di Ricerca di Messina, and Dipartimento di Fisica, Università degli Studi di Messina.

10.1021/jp013150k CCC: $22.00
Published on Web 00/00/0000 PAGE EST: 5.9

method. More recently, GEMC simulations of a highly asymmetric ($q = 0.1$) binary mixture have shown that fluid−fluid phase separation may occur on account of a small amount of nonadditivity,[36] a conjecture that had been already raised by Biben and Hansen.[37] In such a strongly asymmetric regime, another fruitful theoretical approach is based on the calculation of the effective potential between larger particles that is obtained after integrating out the degrees of freedom of smaller spheres.[2,38−41]

As anticipated above, the aim of this work is to extend a previous study on symmetric NAHS mixtures[3] to the asymmetric case in a regime where particle sizes are not too different from unity ($q \geq \mathbf{0}.75$). This model, notwithstanding the crudeness of the representation, contains some basic features that can be used, for example, to sketch the phase behavior of binary fluids at very high pressures (∼1 GPa).[42] Here, we are specifically interested in understanding the interplay between the presence of small degrees of nonadditivity ($\Delta \leq 0.1$) and moderate size asymmetries in triggering fluid−fluid and/or fluid−solid transitions in the mixture. The layout of the paper is as follows: The basic theoretical framework is introduced in section 2, while the numerical simulation technique is described in section 3. A complementary integral-equation approach, based on the approximate Martinov and Sarkysov (MS) closure,[43] is outlined in section 4. Results are discussed in section 5, and section 6 is devoted to concluding remarks.

2. Entropy and Correlations

The total excess entropy can be expanded as an infinite series:[4,7]

$$s_{(\mathrm{ex})} = \sum_{n=2}^{\infty} s_n \tag{1}$$

where $s_{(\mathrm{ex})}$ is the excess entropy per particle in units of the Boltzmann constant k_B and the partial entropies s_n are obtained from the integrated contributions of the spatial correlations between n-tuples of particles. In particular, in a multicomponent system the two-body term can be written as[6]

$$s_2 = -{}^1\!/_2 \rho \sum_{ij} x_i x_j \int \{g_{ij}(r) \ln [g_{ij}(r)] - g_{ij}(r) + 1\}\, \mathrm{d}r \tag{2}$$

where $\rho = \rho_1 + \rho_2$ is the total number density, x_i is the mole fraction of the ith species ($i = 1, 2$), and the quantities $g_{ij}(r)$ are the partial pair distribution functions (PDF). The residual multiparticle entropy (RMPE)

$$\Delta s \equiv s_{(\mathrm{ex})} - s_2 \tag{3}$$

is a sensitive indicator of the structural changes that take place in the system. In fact, at variance with the pair entropy, Δs exhibits a nonmonotonic behavior when plotted as a function of the number density, changing from negative at low densities to positive values at higher densities. The zero-RMPE value [$\Delta s(\rho_0) = 0$] turns out to be systematically correlated with the thermodynamic stability threshold of the homogeneous disordered phase.

To describe the local structure of the mixture, we also resorted to the coordination numbers:

$$n_{ij} = 4\pi\rho x_i \int_{\sigma_{ij}}^{r_{ij}^{\min}} g_{ij}(r) r^2\, \mathrm{d}r \tag{4}$$

where n_{ij} represents the average number of particles of type j surrounding a particle of type i up to the location ($r_{ij}^{\min}$) of the first minimum of $g_{ij}(r)$. More specifically, we made use of the quantities[28]

$$c_{\mathrm{l}} \equiv n_{11}(r_{11}^{\min}) + n_{22}(r_{22}^{\min}) \tag{5}$$

$$c_{\mathrm{u}} \equiv 2n_{12}(r_{12}^{\min}) \tag{6}$$

where c_{l} counts the total number of like species within the first coordination shells of $g_{11}(r)$ and $g_{22}(r)$, while c_{u} represents the total number of unlike species within the first coordination shells of $g_{12}(r)$ and of the symmetrical PDF $g_{21}(r)$. The proximity of the mixture to a fluid−fluid separation point is signaled by a maximum in c_{u}, when this quantity is plotted as a function of the density.[28] Conversely, the monotonic trend of c_{l} is not affected by the impending transition.

3. Monte Carlo Simulation

To generate the partial PDFs we performed extensive constant-temperature MC simulations. We simulated systems with a number of particles ranging from $N = 500$ to $N = 1372$ and used a perfectly ordered face-centered-cubic (FCC) lattice as the starting configuration of the system that was enclosed in a cubic box with periodic boundary conditions. To check the importance of size effects, we also carried out a few runs with 4000 particles. The equilibration period was typically 10^5 to 4×10^6 MC cycles, depending on the density, where an MC cycle consisted of an attempt at changing sequentially the position of each particle. The maximum displacement was varied in order to keep the acceptance ratio of the MC moves between 0.4 and 0.5. The stability of PDF contact values was considered (within the numerical error) a good indication of the equilibration achieved in proximity of the phase-separation threshold. Simulation data were obtained by generating chains consisting of 5×10^5 to 4×10^6 MC cycles. Equilibrium averages and standard deviations were computed by dividing chains into separate independent blocks. During the cumulation runs, we constructed different histograms for the distribution functions that contribute to the pair entropy and to the coordination numbers. Note that at intermediate and high densities a larger number of particles is needed not only to improve the overall statistics but also to extend the spatial range of the distribution functions as much as possible. This requisite is critical in order to obtain a quantitatively reliable estimate of the pair entropy as given by eq 2. We calculated the partial PDFs of an equimolar mixture for $\Delta = 0.01$, 0.03, 0.05, and 0.1 and for $q = 0.75$, 0.85, and 1.00 and spanned the entire concentration range for $\Delta = 0.1$ and $q = 0.75$, 0.85 in order to trace the zero-RMPE locus as an estimate of the thermodynamic stability line. A similar analysis was also performed for $\Delta = 0.05$ and $q = 0.85$.

We calculated the compressibility factor as

$$\frac{\beta P}{\rho} = 1 + {}^2\!/_3 \pi\rho \sum_{ij} x_i x_j \sigma_{ij}^3 g_{ij}(\sigma_{ij}) \tag{7}$$

where P is the pressure and $\beta \equiv (k_B T)^{-1}$ is the inverse temperature in units of the Boltzmann constant. Upon integration, one obtains the excess entropy of the mixture as

$$s_{(\mathrm{ex})}(\rho) = -\int_0^{\rho} \left[\frac{\beta P}{\rho} - 1\right] \frac{\mathrm{d}\rho'}{\rho'} \tag{8}$$

The thermodynamic integration appearing in eq 8 was carried out with a spline approximant of the MC data. As usual with computer simulations close to phase boundaries, one has to

monitor with special care the nature of the system that is being simulated. Indeed, in some thermodynamic states the system starts to phase-separate. However, since the interdiffusion process is usually slow, it may be difficult to timely recognize the onset of two-phase coexistence in the simulation box.

In our study, we monitored systematic variations of the local coordination numbers once the topological equilibration of the sample was safely realized. We evaluated the RMPE for homogeneous states only or for a few states marginally inside the two-phase region. In this latter case, the estimate of the RMPE should be considered as a kind of transient estimate.

4. Integral Equations

The Ornstein−Zernike (OZ) integral equation for mixtures reads

$$h_{ij}(r) + c_{ij}(r) + \sum_k \rho_k \int h_{ik}(r')c_{ik}(|r - r'|)\, dr' \qquad (9)$$

where h_{ij} and c_{ij} are the total and the direct correlation functions, respectively. A closure relationship is introduced when a functional form is given for $g_{ij}(r)$. In general, one can write

$$g_{ij}(r) \equiv 1 + h_{ij}(r) \equiv \exp[\beta u_{ij}(r) + \omega_{ij}(r)] \qquad (10)$$

where $u_{ij}(r)$ is the interaction potential. The MS closure corresponds to

$$\omega_{ij}(r) = [1 + 2\gamma_{ij}(r)]^{1/2} - 1 \qquad (11)$$

In this case we limit ourselves to the exploration of the instability associated with the spinodal curve. We solved the integral equation using the method originally proposed by Gillan with 1024 equally spaced grid points, setting the mesh size to 0.01.[44] After solving the OZ equation, we evaluated the Bhatia−Thornton structure factor $S_{cc}(k)$ through the following relation:[25]

$$S_{cc}(k) \equiv x_1x_2[x_2S_{11}(k) + x_1S_{22}(k) - 2(x_1x_2)^{1/2}S_{12}(k)] \qquad (12)$$

where k is the wavenumber and $S_{ij}(k)$ are the partial structure factors:

$$S_{ij}(k) \equiv \delta_{ij} + (x_1x_2)^{1/2}\rho\tilde{h}_{ij}(k) \qquad (13)$$

Here δ_{ij} is the Kronecker delta and $\tilde{h}_{ij}(k)$ are the Fourier transforms of the total correlation functions. In particular

$$S_{cc}(k = 0) = N\langle(\Delta x)^2\rangle = Nk_BT\left(\frac{\partial^2 G}{\partial x^2}\right)^{-1}_{T,P,N} \qquad (14)$$

where G is the Gibbs potential. We plotted the ratio $(x_1x_2)/S_{cc}(0)$ as a function of the number density ρ. The value at which this quantity vanishes is taken as an approximate estimate of the spinodal point.

5. Results

5.1. Equimolar Mixtures. We start by discussing the properties of an equimolar mixture ($x_1 = x_2 = {}^1/_2$) so as to highlight the effects associated with size asymmetry and nonadditivity only. We first present the RMPE for different values of the size ratio and of the nonadditivity parameter. Figure 1a shows the density dependence of this quantity. As already noted elsewhere, the position of the minimum in the RMPE identifies a structural threshold beyond which the system enters a liquidlike regime where cooperative, i.e., intrinsically many-body, effects come into play in determining the state of the fluid.[5,8]

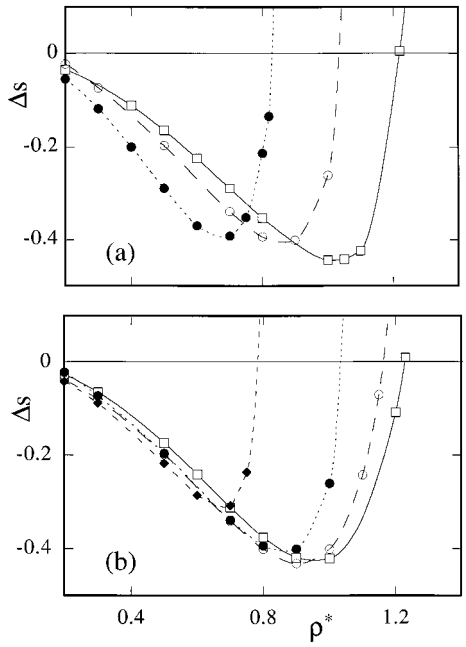

Figure 1. Residual multiparticle entropy plotted as a function of the reduced number density for (a) $\Delta = 0.05$ and $q = 0.75$ (0), q = 0.85 (O), and q = 1 (b); (b) q = 0.85 and D = 0 (0), D = 0.03 (O), D = 0.05 (b), and D = 0.1 ([). The data for D = 0 are from ref 6. Lines are a guide for the eye.

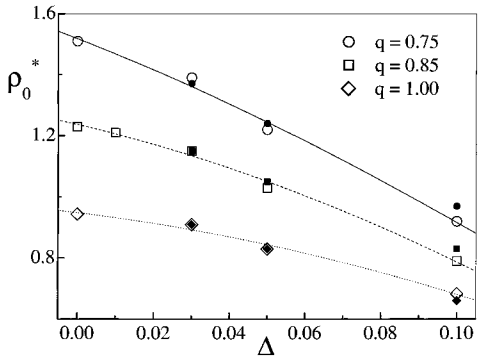

Figure 2. Zero-RMPE reduced densities plotted as a function of Δ for equimolar mixtures: (O) q = 0.75, (0) q = 0.85, and (]) q = 1. The solid markers are the corresponding estimates of the spinodal points produced by the MS integral-equation closure. Lines are a guide for the eye.

In the following, we shall use reduced units for the number density: $\rho^* = \rho\sigma_{11}{}^3$. The zero-RMPE density ρ_0^* was found to increase for decreasing values of the size ratio. Vice versa, upon increasing the value of the nonadditivity parameter while keeping fixed the size ratio, ρ_0^* decreases (see Figure 1b). A synthesis of these results is given in Figure 2.

As shown by the above analysis, the phase behavior of the mixture is sensitively tuned by the size ratio and by the nonadditivity parameter. However, we recall that the one-phase character of the zero-RMPE criterion does not allow for an exact characterization of the phase transition occurring in the vicinity of ρ_0^*. Indeed, within such a framework we cannot easily detect what kind of phase transition the mixture undergoes. To get an independent clue on this, we also evaluated the coordination numbers for both like and unlike species.

Figure 3 shows how c_l and c_u change with the density: c_l increases monotonically with the density, irrespectively of the

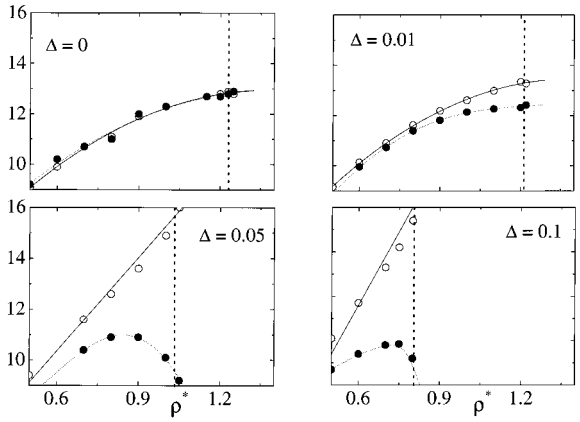

Figure 3. Like and unlike coordination numbers as defined by eqs 5 and 6, plotted as a function of the reduced number density for $q = 0.85$: (O) cl; (b) cu. Lines are a guide for the eye.

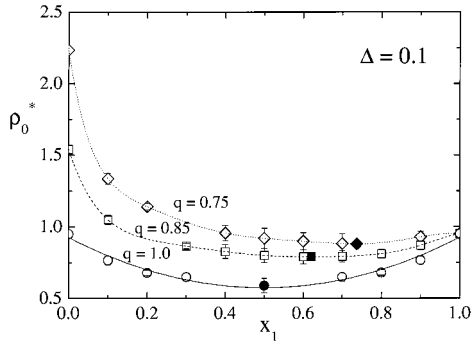

Figure 4. Zero-RMPE thresholds of a NAHS mixture plotted as a function of the larger-sphere mole fraction for $\Delta = 0.1$ and $q = 1$ (O), $q = 0.85$ (0), and $q = 0.75$ (]). The corresponding solid markers locate the minimum of each zero-RMPE locus. Estimated error bars are also indicated. Lines are a guide for the eye.

value taken by the nonadditivity parameter and at variance with c_u, whose behavior changes in a distinct way upon increasing the value of Δ. In fact, for $\Delta = 0$, this latter quantity shows the same trend as c_l, a rather clear indication of the fact that, consistently with independent numerical simulation experiments,[11] the system will eventually undergo a transition to a substitutionally disordered FCC phase. For $\Delta = 0.01$, the two curves tend to branch off while still preserving a monotonic trend. However, upon further increasing the nonadditivity parameter, a broad peak develops in c_u, located at a value of ρ^* that is close to the vanishing threshold of the RMPE: the gradual drop of c_u at high densities signals that the system is likely experiencing a different phase transition that is characterized by a tendency of differently sized particles to segregate. We note, in passing, that the average number of particles lying around a central reference one, irrespectively of the species, grows monotically, also for nonzero values of the nonadditivity parameter, to values slightly larger than 12 at the transition point.[9]

5.2. Concentration Effects. We now explore the phase behavior of the mixture as a function of the molar composition. Figure 4 shows the zero-RMPE locus for $\Delta = 0.1$ and for three values of the size ratio. A difference in the like diameters obviously induces an asymmetry of the curve. Hence, estimating the critical density (and, correspondingly, the critical composition) becomes more and more difficult, requiring very long simulation runs about the minimum of the curve. We observe that, upon increasing the asymmetry of the two species, the estimated critical composition increases as also does the critical density.

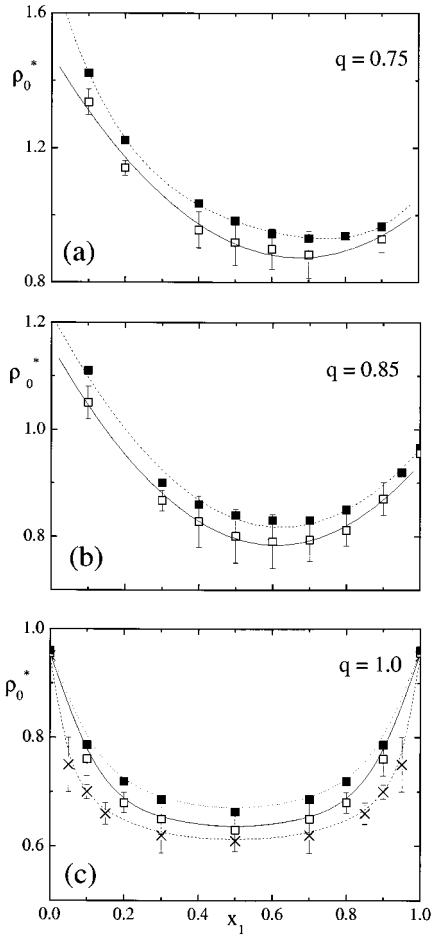

Figure 5. Comparison between zero-RMPE estimates (0) and MS spinodal densities (9) for $\Delta = 0.1$ and (a) $q = 0.75$, (b) $q = 0.85$, and (c) $q = 1$. GEMC coexistence densities are also plotted for the symmetric mixture.[35] Estimated error bars are also indicated. Lines are a guide for the eye.

A comparison with the MS prediction of the spinodal curve and with the currently available simulation data for the coexistence line of the symmetric mixture is presented in Figure 5. The qualitative agreement between the integral-equation results and the zero-RMPE locus is fairly good over the whole range of mole fractions. Indeed, it turns out that the zero-RMPE thresholds fall systematically below the spinodal line predicted by the MS closure. In this respect, we note that the MS closure was tested for a similar system against the GEMC simulation results.[35] Here, the authors remarked that the closure, while being rather accurate in describing the structural properties of the homogeneous liquid phases, slightly overestimates the simulation results for the critical parameters (see Figure 5). Very recently, the MS closure was also implemented in order to study the fluid−fluid phase equilibrium of a NAHS mixture adsorbed within a frozen disordered hard-sphere matrix.[45] A comparison with the MC data led the authors to conclude that the MS approximation works systematically better than other approximate closures of the reference OZ equation.

An even more illuminating perspective is offered by Figure 6, which shows the effect of increasing nonadditivities on the behavior of the zero-RMPE density when this quantity is plotted as a function of the mole concentration of the larger particles. In the additive mixture the curve is monotonic: in this case, the profile is just feebly modified with respect to a linear law that merely interpolates between the freezing thresholds of the pure components. Note, in this respect, that the reduced density

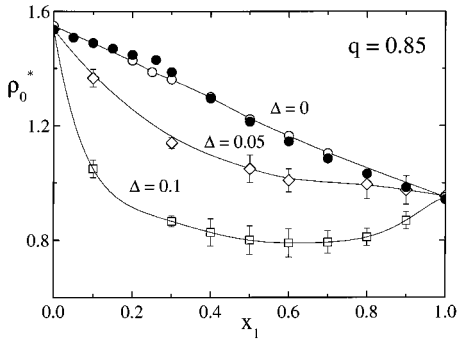

Figure 6. Zero-RMPE thresholds of a NAHS mixture for $q = 0.85$ and $\Delta = 0$ (O), D = 0.05 (]), and D = 0.1 (0). The data for $\mathbf{\Delta} = 0$ are from ref 6. Solid circles represent the freezing densities of an additive hard-sphere mixture as calculated in ref 11.

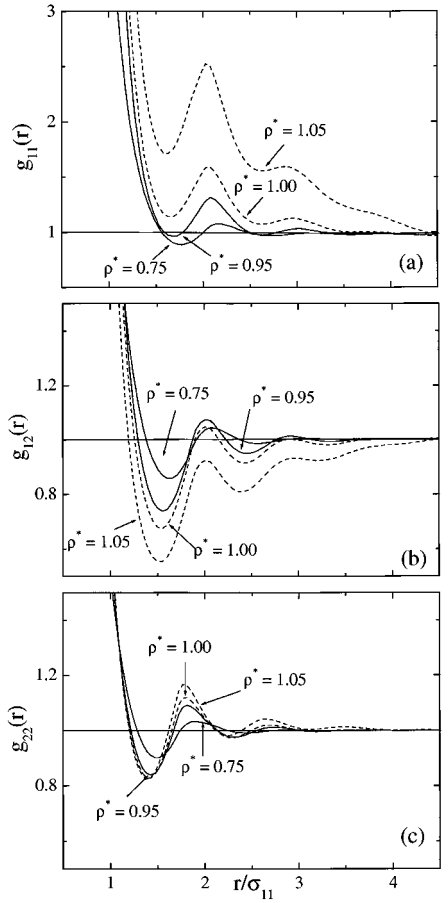

Figure 7. Density evolution of the pair distribution functions of a NAHS mixture for $q = 0.85$, $\Delta = 0.1$, and $x_1 = 0.1$. Dotted lines refer to densities just larger than the zero-RMPE threshold value $\rho_0^* = 1.04$.

is expressed in terms of the larger-particle diameter. However, as soon as even weak nonadditive interactions between unlike particles are switched on, the overall profile is rather severely modified and the ordering threshold progressively moves to lower and lower densities since the extra excluded-volume interactions do actually favor an anticipated (with respect to the additive case) ordering of the mixture. At this stage, also for continuity with the pure case, we expect that the denser species will likely crystallize while the other component will concurrently segregate, forming disordered clusters. This structural scenario seems consistent with the local density profiles that are shown in Figure 7 for an asymmetric ($q = 0.85$) and nonadditive ($\Delta = 0.1$) mixture with molar composition $x_1 = 0.1$. In this case, the ordering threshold estimated through the

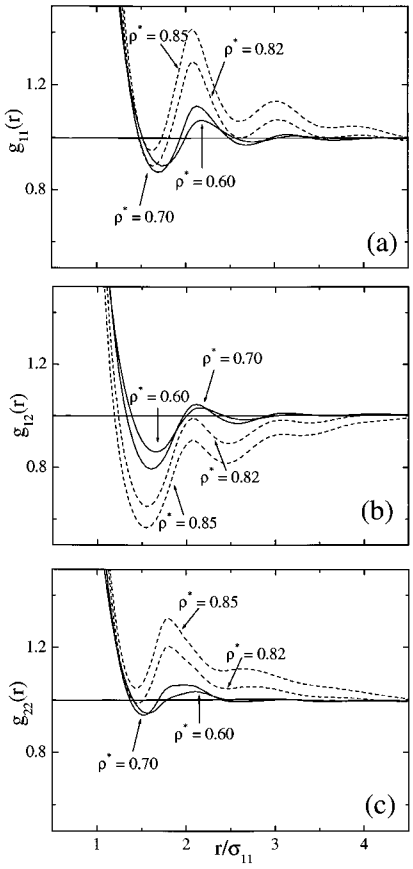

Figure 8. Density evolution of the pair distribution functions of a NAHS mixture for $q = 0.85$, $\Delta = 0.1$, and $x_1 = 0.4$. Dotted lines refer to densities just larger than the zero-RMPE threshold value $\rho_0^* = 0.82$.

vanishing of the RMPE is $\rho_0^* = 1.04$, a value rather close to the MS prediction of the thermodynamic stability border of the homogeneous mixture (see Figure 5). At low densities the three PDFs oscillate about unity with a more or less standard behavior. However, as soon as the mixture is compressed to densities larger than ρ_0^*, the shapes of both $g_{11}(r)$ and $g_{12}(r)$ do visibly change in a rather anomalous way: in fact, the larger-particle PDF shows a profile that seems consistent with an amorphous accretion of like particles around a central one in that even at less favored positions (the minima) lies, on average, a considerable fraction of particles. Concurrently, the coordination shell of a given particle is progressively emptied from unlike particles (see also Figure 3). Note also that not only does the contact value $g_{12}(\sigma_{12})$ decrease with increasing densities but also the local density at medium and large distances is progressively depressed below the average macroscopic value. On the other hand, the profile of the smaller-particle PDF just shows more enhanced and longer-ranged oscillations about unity, which are plausibly consistent with the incipient nucleation of a solid cluster as is typical of a pure fluid.

For large enough nonadditivities, the ordering threshold associated with the vanishing of the RMPE eventually drops even below the freezing density of the larger particles and, as a result, a minimum develops. In this case, we argue that the nature of the ordering mechanism undergone by the mixture in the concentration range where $\rho^* < 0.95$ gradually changes. For densities larger than the RMPE-ordering threshold ($\rho_0^* = 0.82$), the like PDFs of the same model mixture discussed above but for a more symmetrical molar composition ($x_1 = 0.4$) do show a similar behavior (see Figure 8). The overall structural information indicates that the mixture will eventually undergo

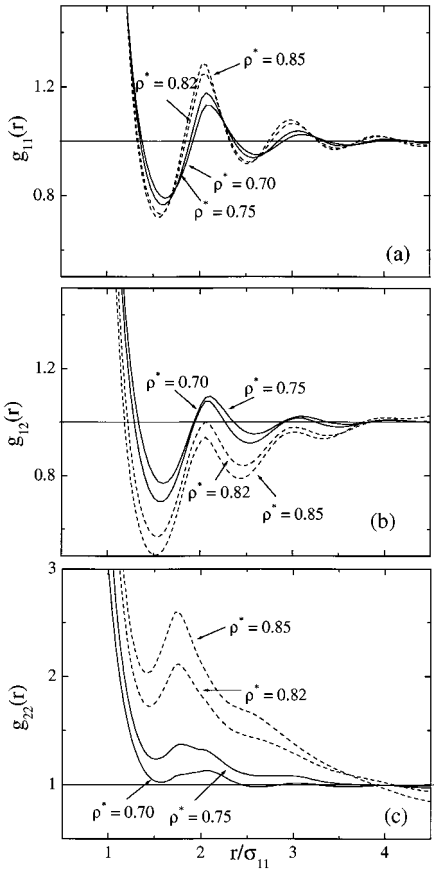

Figure 9. Density evolution of the pair distribution functions of a NAHS mixture for $q = 0.85$, $\Delta = 0.1$, and $x_1 = 0.8$. Dotted lines refer to densities just larger than the zero-RMPE threshold value $\rho_0^* = 0.81$.

a fluid−fluid separation instead of an even partial freezing. The composition range within which demixing is likely to occur sensitively depends on the size ratio of the two species, as also shown in Figure 4. For largely asymmetric mixtures, fluid−fluid separation is expected to become eventually metastable with respect to freezing.[37,36]

Figure 9 shows the PDFs in the opposite concentration regime, i.e., for $x_1 = 0.8$. Here the situation is somewhat specular to that previously analyzed for $x_1 = 0.1$, but for the fact that it is now the larger particles that visibly prearrange for solidification while the smaller ones tend to cluster in a more or less disordered way.

6, Concluding Remarks

In this paper we have presented Monte Carlo results on the thermodynamic and structural properties of a moderately asymmetric mixture of hard spheres with weakly nonadditive repulsive interactions. The corresponding range of values attained by the parameters of the model ($0.75 \leq q \leq 1$; $0 \leq \Delta \leq 0.1$) is such that fluid−fluid phase separation does in fact compete with the fluid−solid transition. To estimate the location of the intrinsic structural stability thresholds, we calculated the residual multiparticle entropy whose zero is a very sensitive indicator of the incipient ordering of the homogeneous fluid mixture, as is also confirmed by a comparison with the spinodal boundaries that are predicted by an approximate but quite reliable integral-equation closure. This one-phase analysis was corroborated with the calculation of the like and unlike coordination numbers, which, together with the parent radial distribution functions, provide useful hints on the nature of the higher-density phase. We found that the thermodynamic behavior of the mixture depends in a very sensitive way on the degree of nonadditivity, which, together with the size ratio of the two species, finely tunes the character of the thermodynamic transition eventually undergone by the mixture from an even partial solidification to a fluid−fluid phase separation.

References and Notes

(1) Rowlinson, J. S. *Liquids and liquid mixtures*; Butterworth: London, 1969.

(2) Louis, A. A. *Philos. Trans. R. Soc. London A* **2001**, *359*, 939.

(3) Saija, F.; Pastore, G.; Giaquinta, P. V. *J. Phys. Chem. B* **1998**, *102*, 10368.

(4) Nettleton, R. E.; Green, M. S. *J. Chem. Phys.* **1958**, *29*, 1365.

(5) Giaquinta, P. V.; Giunta, G. *Physica A* **1992**, *187*, 145.

(6) (a) Saija, F.; Giaquinta, P. V.; Giunta, G.; Prestipino, G. S. *J. Phys.: Condens. Matter* **1994**, *6*, 9853. (b) Saija, F.; Giaquinta, P. V. *J. Phys.: Condens. Matter* **1996**, *8*, 8137.

(7) (a) Prestipino, S.; Giaquinta, P. V. *J. Stat. Phys.* **1999**, *96*, 135. (b) Prestipino, S.; Giaquinta, P. V. *J. Stat. Phys.* **2000**, *98*, 507.

(8) Saija, F.; Prestipino, S.; Giaquinta, P. V. *J. Chem. Phys.* **2000**, *113*, 2806.

(9) Saija, F.; Prestipino, S.; Giaquinta, P. V. *J. Chem. Phys.* **2001**, *115*, 7586.

(10) Frenkel, D. *J. Phys.: Condens. Matter* **1994**, *6*, A71−A78.

(11) Kranendonk, W. G. T.; Frenkel, D. *Mol. Phys.* **1991**, *72*, 679.

(12) Denton, A. W.; Ashcroft, N. W. *Phys. Rev. A* **1990**, *42*, 7312.

(13) Eldridge, M. D.; Madden, P. A.; Frenkel, D. *Nature* **1993**, *365*, 35.

(14) Biben, T.; Hansen, J. P. *Phys. Rev. Lett.* **1991**, *66*, 2215.

(15) (a) Dijkstra, M.; van Roij, R.; Evans, R. *Phys. Rev. Lett.* **1998**, *81*, 2268. (b) Dijkstra, M.; van Roij, R.; Evans, R. *Phys. Rev. Lett.* **1999**, *82*, 117. (c) Dijkstra, M.; van Roij, R.; Evans, R. *Phys. Rev. E* **1999**, *59*, 5744.

(16) Albas, P.; van der Marel, C.; Geertsman W.; Meijer, J. A.; van Osten, A. B.; Dijkstra, J.; Stein, P. C.; van der Lugt, W. *J. Noncrystalline Solids* **1984**, *61/62*, 201.

(17) Gazzillo, D.; Pastore, G.; Enzo, S. *J. Phys.: Condens. Matter* **1989**, *1*, 3469.

(18) Gazzillo, D.; Pastore, G.; Frattini, R. *J. Phys.: Condens. Matter* **1990**, *2*, 8463.

(19) Tenne, R.; Bergmann, E. *Phys. Rev. A* **1978**, *17*, 2036.

(20) Mazo, R.; Bearman, R. J. *J. Chem. Phys.* **1990**, *93*, 6694.

(21) Barboy, B.; Gelbart, W. N. *J. Chem. Phys.* **1979**, *71*, 3053.

(22) Barboy, B.; Gelbart, W. N. *J. Stat. Phys.* **1980**, *22*, 709.

(23) Nixon, J. H.; Silbet, M. *Mol. Phys.* **1984**, *52*, 207.

(24) Ballone, P.; Pastore, G.; Galli, G.; Gazzillo, D. *Mol. Phys.* **1986**, *59*, 275.

(25) Gazzillo, D. *J. Chem. Phys.* **1991**, *95*, 4565.

(26) Lomba, E.; Alvarez, M.; Lee, L. L.; Almarza, N. E. *J. Chem. Phys.* **1996**, *104*, 4180.

(27) Saija, F.; Fiumara, G.; Giaquinta, P. V. *J. Chem. Phys.* **1998**, *108*, 9098.

(28) Jung, J.; Jhon, M. S.; Ree, F. H. *J. Chem. Phys.* **1995**, *102*, 1349.

(29) Hamad, E. Z. *J. Chem. Phys.* **1996**, *105*, 3222.

(30) Hammawa, H.; Hamad, E. Z. *J. Chem. Soc., Faraday Trans.* **1996**, *92*, 4943.

(31) Melnyk, T. W.; Sawford, B. L. *Mol. Phys.* **1975**, *29*, 891.

(32) Adams, D. J.; McDonald, I. R. *J. Chem. Phys.* **1975**, *63*, 1900.

(33) Gazzillo, D.; Pastore, G. *Chem. Phys. Lett.* **1989**, *159*, 388.

(34) Amar, J. G. *Mol. Phys.* **1989**, *67*, 739.

(35) Rovere, M.; Pastore, G. *J. Phys.: Condens. Matter* **1994**, *6*, A163.

(36) Dijkstra, M. *Phys. Rev. E* **1998**, *58*, 7523.

(37) Biben, T.; Hansen, J.-P. *Physica A* **1997**, *235*, 142.

(38) Louis, A. A.; Finken, R.; Hansen, J.-P. *Phys. Rev. E* **2000**, *61*, R1028.

(39) Roth, R.; Evans, R. *Europhys. Lett.* **2001**, *53*, 271.

(40) Louis, A. A.; Roth, R. Preprint cond-mat/0102049.

(41) Roth, R.; Evans, R.; Louis, A. A. Preprint cond-mat/0105547.

(42) Shouten, J. A. *Int J. Thermophys.* **2001**, *22*, 23.

(43) Martynov, G. A.; Sarkisov, G. N. *Mol. Phys.* **1983**, *49*, 1495.

(44) Gillan, M. J. *Mol. Phys.* **1979**, *38*, 1781.

(45) Sierra, O.; Duda, Y. *Phys. Lett. A* **2001**, *280*, 146.